FATIGUE OF IMPACT-DAMAGED CARBON FIBRE COMPOSITES

by G. Clark and T.J. van Blaricum

Presented at the XXI OSTIV Congress, Wiener-Neustadt, Austria (1989)

SUMMARY

The sensitivity of carbon and glass fibre composite aircraft materials to low-level impact damage leads to some concern about possible long-term degradation of these materials by fatigue, particularly under compressive loading. As for metals, the testing of these materials must be carried out under realistic flight by flight loading, and for composites such testing is complicated by the fact that these materials display good fatigue properties combined with a higher level of scatter than for metals. The duration of fatigue tests can be much greater than for metals, and the testing techniques considerably more complex due to the need to test using predominatly compressive loading. This paper investigates the effects of using a modified loading spectrum to accelerate fatigue testing of carbon-fibre composite laminates, examines the growth rates of realistic impact damage in tests which represent flight by flight loading of an aircraft wing, and discusses briefly some of the problems associated with compression fatigue testing of composites.

1. Introduction

The use of glass and carbon fibre composites in aircraft primary structure (an application which was pioneered by the designers of glass fibre sailplanes in Germany) has increased rapidly in recent years because these materials offer strength to weight ratios which are substantially better than for metals. One result of this has been an increased interest in the durability and damage tolerance of composite materials.

Of special concern is barely-visible impact damage (BVID) resulting from a low energy impact (typically 3 to 20 J) as might be caused by tool drops or runway stones, in military and civil aircraft, and mishandling during rigging or transportation where composite glider structures are concerned. Such impacts produce internal damage (inter-ply delaminations and ply cracking), leaving little evidence of damage on the impacted surface. BVID has little effect on tensile strength, although compressive strength can be reduced considerably by the initial impact; BVID could, therefore, lead to immediate structural failure in very highly stressed components, and the possibility of failure as a result of damage growth during fatigue loading must also be considered. This is particularly important for wing upper surfaces, which are especially prone to damage and also experience compressive flight loads. Moisture absorption (1) is also known to degrade the mechanical properties of composites.

The effect of an idealised single delamination on static compression strength has been the subject of theoretical work (e.g. refs. 2-6) and a number of experimental studies (e.g. refs. 2, 7), and is now fairly well understood. However, the behaviour under load of the complex mixture of delaminations and cracking which results from real impact damage has been less extensively studied (examples are refs. 8-10).

Figure 1 is a schematic representation of the way that impact damage reduces the static and fatigue strengths of CFC composite laminates. As damage size increases, the static compressive strength decreases, at first rapidly and then more slowly, towards a value of approximately half the undamaged strength (11-13). At strains less than this "static threshold" value, immediate static failure will not occur. However, as shown in Figure 1, both constant amplitude and spectrum fatigue can produce failure from BVID at significantly lower strains (11, 13); a "fatigue threshold," below which an essentially infinite fatigue life is obtained, exists at approximately 60% of the "static threshold" and represents the lower boundary of an (as yet poorly defined) fatigue failure regime.

Figure 1 also shows the way a conventional S-N representation of fatigue performance is associated with any particular case of BVID; for short fatigue lives, peak fatigue stresses approaching the static threshold are necessary, while for stresses near the fatigue threshold, lives of 10^6 to 10^7 cycles are obtained, whether or not any particular example of BVID

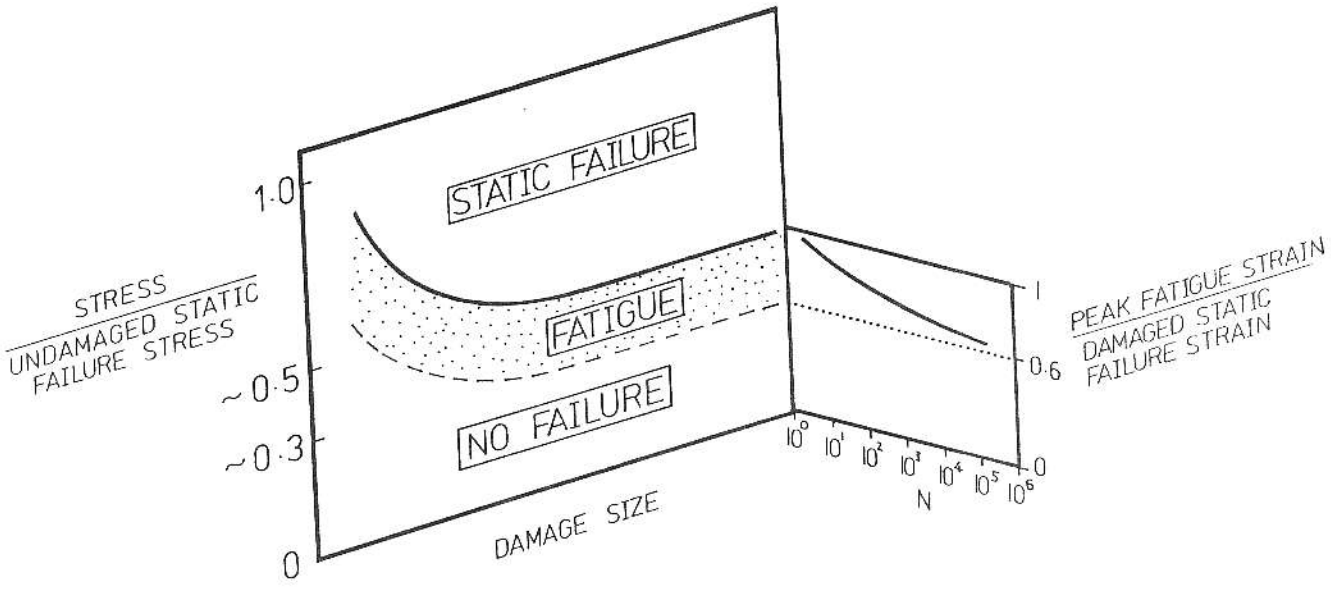

Figure 1. Schematic representation of the effect of increasing size of BVID on the (compressive) static and fatigue properties of CFC laminates, based on data from refs. (18) and (23) and others. The "static failure" regime indicates conditions which produce immediate static failure, the "fatigue regime" marked shows the range of peak fatigue strains which will produce fatigue failure, and the right-hand figure shows the S-N behaviour appropriate to each specific size of impact damage.

is a potential fatigue problem may be determined from the fatigue threshold strain for that particular laminate and spectrum; if the aircraft operates at peak strains above the fatigue threshold, knowledge of the S-N behaviour in Figure 1, or damage growth rates, is required to estimate an appropriate fatigue life for the component.

The way in which impact damage grows in the fatigue regime of Figure 1 has received only limited attention, particularly for the case of realistic aircraft spectrum loading. This is due in part to the complex procedures required for fatigue testing under compressive loads and to the fact that composites normally show more scatter in mechanical properties than metals, and hence require greater numbers of tests. This is exacerbated by the need to avoid high test frequencies to limit heating which might degrade the resin properties. A further complicating factor was suggested by Heath-Smith (14), who observed that fatigue damage accumulation at high loads in the spectrum may occur more rapidly than at the lower loads. If confirmed, this observation is of direct interest in relation to aircraft operating conditions, and also because it raises the possibility that simply deleting the "low damage" loads might lead to dramatic reductions in testing time, without significantly affecting component fatigue behaviour. The benefits of such reduction would be especially valuable in expensive and complex tests on large components, or entire aircraft.

The aim of aircraft structural testing under realistic flight by flight loading is to verify the design procedures used and to identify fatigue critical areas. For mixed metal/composite structures, however, development of a test which adequately interrogates both the metal and the composite components is difficult; composites tend to display flatter fatigue S-N behaviour than metals, and furthermore, the rapid fatigue damage accumulation reported for composites at high stresses (c.f. at low stresses in metals) makes any comparison of metal and composites fatigue performance difficult.

One approach which shows some promise *makes use* of the different fatigue damage accumulation sensitivities of metals and composites, as discussed above. If the low loads which are more damaging for metals cause little damage in composite material, it should be possible to develop a compromise load spectrum which produces similar rates of damage accumulation in both metals and composites, thus avoiding the problem of premature failure of metal components.

The work described in this paper is part of a larger program which has the aim of improving our understanding of the damage tolerance of aircraft CFC components. The aspects investigated here are:

(i) whether or not impact damage in an aircraft CFC laminate wil grow under realistic flight-by-flight loading, and the characteristics of any growth;

(ii) whether it is possible to conduct accelerated fatigue tests by deleting low loads from the spectrum, without affecting specimen fatigue life;

(iii) the effects of test fixture design on the performance of composite coupons under compression loading;

(iv) the effect of omittng a post-cure heat-treatment on the fatigue performance of a carbon fibre composite laminate.

2. Experimental

2.1 Test Specimens

The three panels (designated FG, FH and FI) used for test specimens were manufactured at ARL from Ciba-Geigy XAS-914C carbon fibre pre-impregnated sheet. A 56-ply lay up of $[\pm 45/O_2]_{7s}$ representative of a fighter aircraft wing skin was used. The manufacturers recommended cure cycle was used, panels FH and FI also being given a post-cure heat treatment. Eighteen coupons, 300 × 100 mm were cut from each panel, the long axis of the coupons being the 0 degree fibre direction. The material's static compressive strength was estimated from small specimens cut from the undamaged grip area of broken coupons (17).

All coupons were non-destructively inspected using an automated ultrasonic C-scan technique (15, 16) which is capable of establishing and displaying the depth location of any defects, as well as their in-plane location.

The center of each coupon was impacted, using the technique described in section 2.2. After further non-destructive inspection, coupons were stored in sealed bags or at −18 degrees C in order to reduce the absorption of atmospheric moisture which can influence composite compression properties. Weighing of "traveller" specimens showed that the moisture content of the coupons, as tested, was about 0.14%; this is unlikely to have a significant influence on laminate mechanical properties.

2.2 Impact Damage

Specimens to be impact damaged were selected at random from the panel area. The rig used to introduce the damage (Figure 2) has been described in detail elsewhere (11). Briefly,

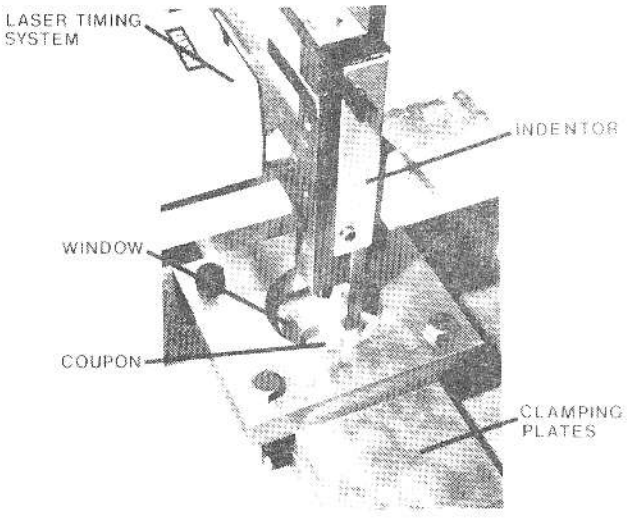

Figure 2.

Rig used to produce low-level impact damage in composite coupons.

a falling mass indentor with a 12.7mm diameter hemispherical thick steel nose was used to impact the center of the coupon, which was clamped between thick steel plates containing a circular "window" in which the laminate was unsupported. This arrangement ensured that the coupons were nominally identical at the beginning of the test. Three different window sizes were used (20, 30 and 40mm diameter). Incident and absorbed impact energies were determined by measuring the incident and rebound velocities of the indentor, using a laser timing system. A constant level of incident impact energy ($12.20 \pm 0.09j$) was used, based on experience with earlier trials (11). This produced minor back face cracking in the form of splitting parallel to the fibers in the surface ply, but left no significant evidence of impact on the front (impact) face. The mean absorbed energies measured were $8.26 \pm 0.19j$ (20mm), $8.11 \pm 0.21j$ (30mm) and $8.18 \pm 0.47j$ (40mm), the low level of scatter indicating that the clamping constraint was consistent. There was no significant influence of window size on absorbed energy, nor did the absence of a post-cure heat-treatment for panel FG have an effect on the impact response of that panel. Non-destructive inspection (NDI) of the samples (Figure 3) showed that the extent of the delamination damage was always close to the window size, and that the damage envelope approximated a truncated cone whose base was located at the back face of the coupon.

2.3 Testing Techniques

Fatigue testing of CFC coupons at high levels of compressive stress requires considerable attention to detailed design of test fixtures, particularly where relatively large gauge areas are needed to simulate realistic service conditions. Initially, various specimen support systems used elsewhere for compression testing were evaluated. None of these fixtures was considered satisfactory, since they all tended to create unacceptably high strains at the end of the specimen gauge area by concentrating any residual testing machine misalignment. The fixture shown in Figure 4 was, therefore, developed; this system (11) also avoids the use of bonded tabs which introduce unwanted residual stresses and complicate specimen alignment procedures. By holding the coupon in hydraulic grips between pairs of high-strength steel plates, load transfer to the specimen occurs via fine serrations on the inner plate surfaces, and an open-weave abrasive-coated loth interlayer. Figure 4 shows the integral grip plate columns which permit attachment of a variety of anti-buckling supports.

For 56-ply coupons, only light edge restraint was required to eliminate gross specimen buckling up to 120% of the required test loads. Figure 5, however, illustrates that for thinner 24-ply material (11), the amount of support significantly affects the apparent static strength of the coupon; very high

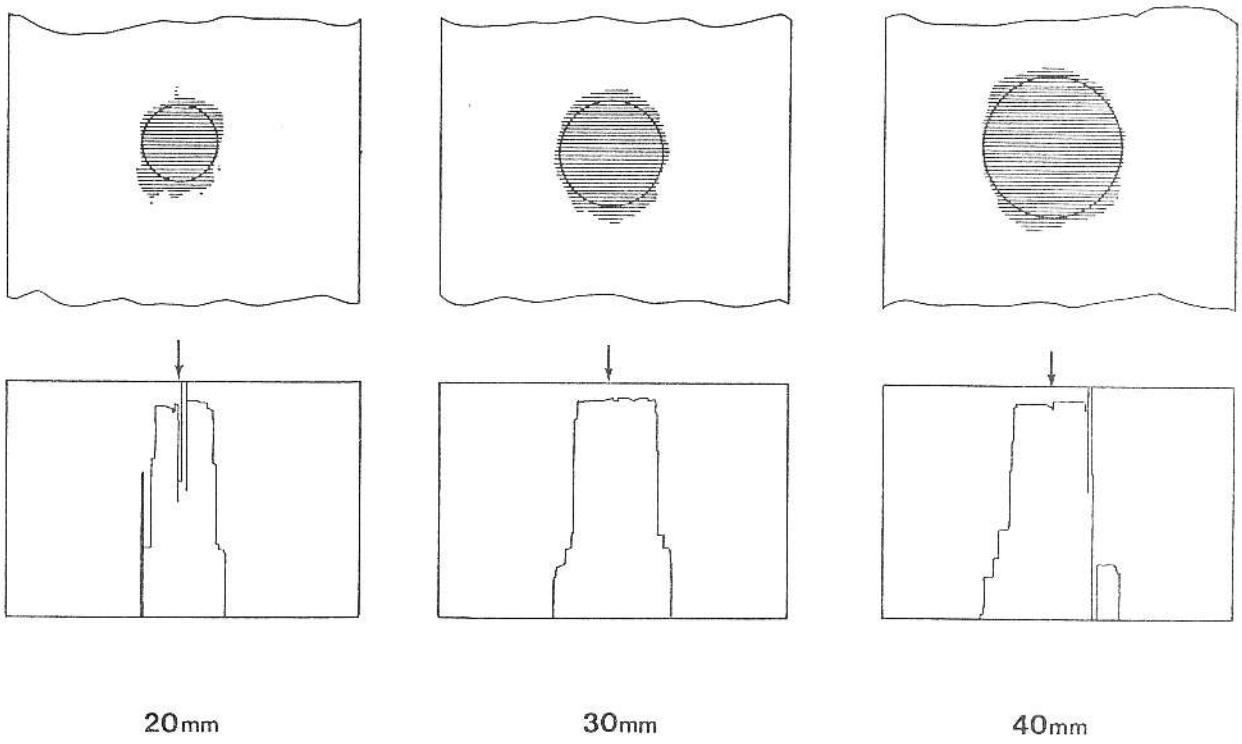

Figure 3. Ultrasonic C-scan records for 20,30 and 40mm diameter damage (upper figures); the size of the window in the impact rig clamping plates is shown. The lower part of the figure displays sections through the centers of the damaged region, showing the damage envelope. The impact position is arrowed.

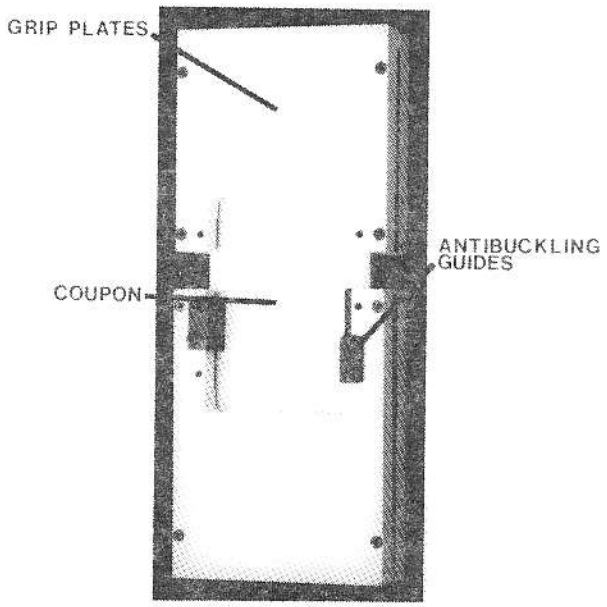

Figure 4.

Test fixture used in compression testing, showing grip plates and antibuckling guides.

levels of constraint were required to achieve consistent results near 900 MPa compressive strength. The amount of constraint used must therefore, be selected with particular care; when the specimen contains impact damage, out of plane movement of the material adjacent to the damage must be permitted if realistic conditions are to be achieved. Testing machine alignment is another critical aspect of this type of testing; misalignment of 0.2mm can produce bending strains of 200 microstrain in coupons of the size tested here. During the ARL test program, alignment of better than 0.08mm was maintained.

2.4 Damage Size Monitoring

Damage size monitoring during the tests was based on the shadow Moire technique, in which the specimen surface, painted white to increase contrast, was illuminated at 45 degree angle of incidence through an optical grid of 10 lines/mm density which was held close (and parallel) to the surface. When the specimen was loaded and viewed normal to the surface through the same grid, any out-of-plane deflection of the surface appears as a series of interference fringes representing approximately 0.15mm deflection per fringe. The deformation visible on the back face in the damaged region could be used to estimate the size of the underlying delamination damage. In practice, the fatigue test was halted at regular intervals at load level 23 (well under the test maximum of level 32) and the fringe pattern was photographed; dimensions of the delamination were then measured from a low-order fringe on the photographs using a computer-linked digitising table.

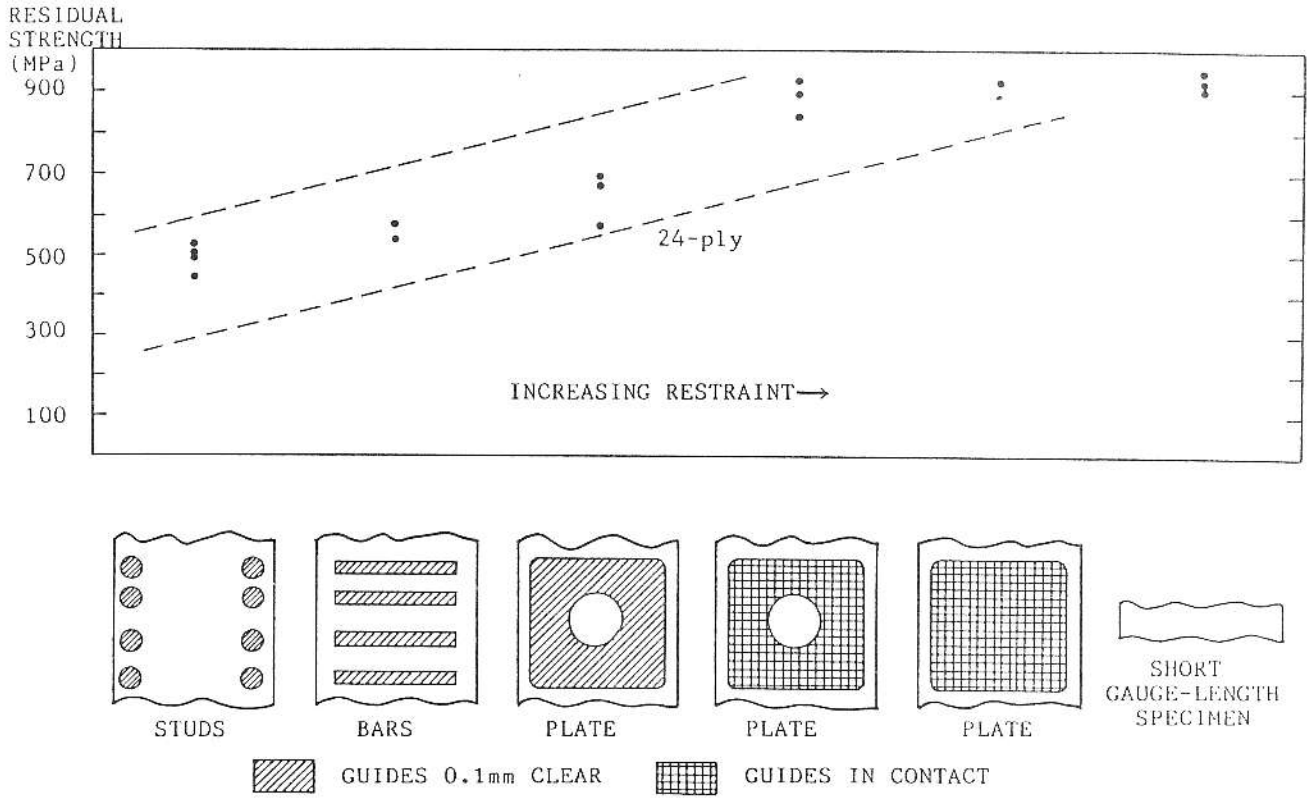

Figure 5. The effect of increasing the level of antibuckling constraint on the compressive failure strength of 24-ply coupons (18).

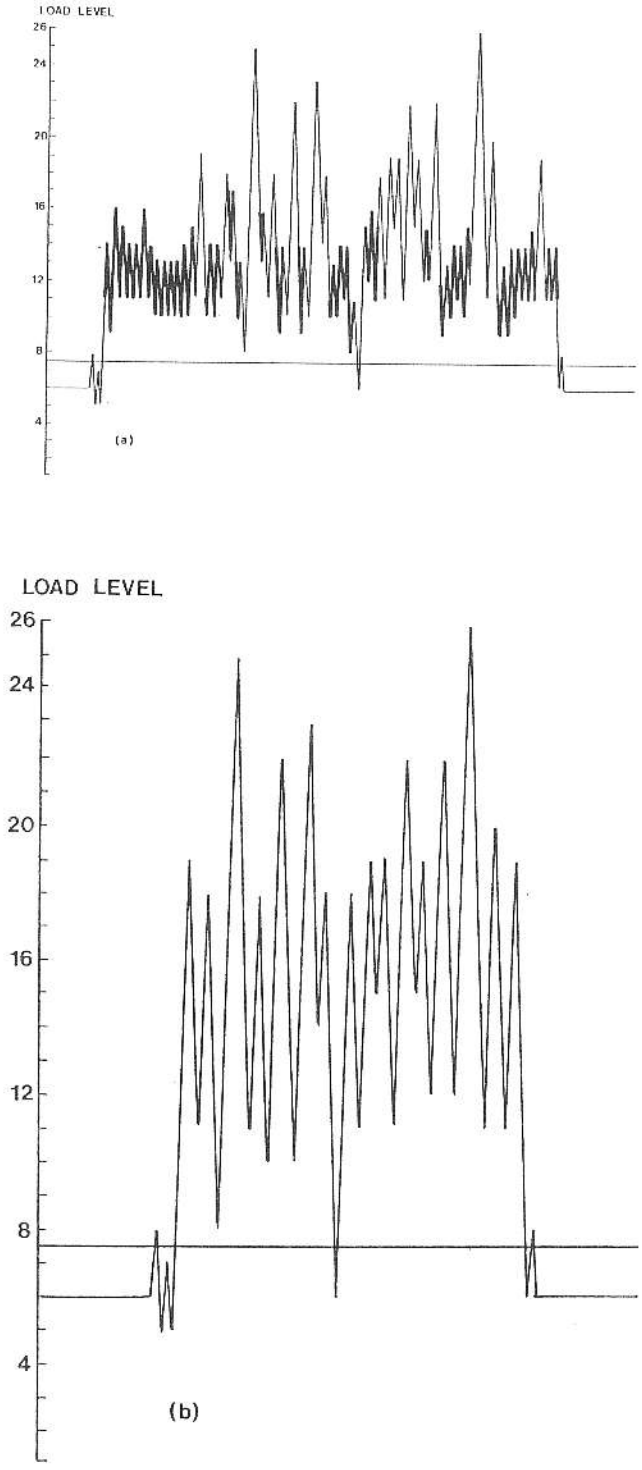

Figure 6. (a) (b)

Flight 13 from full FALSTAFF load sequence, showing cycles (emphasized) deleted during spectrum modification. The zero stress level is marked. (b) Flight 13 from the modified load sequence.

2.5 Load Spectrum

Specimen fatigue loading was based on the FALSTAFF (18) fighter aircraft sequence, which was inverted to provide a compression-dominated spectrum representing upper wing skin service conditions. The load sequence was generated at approximately 10Hz from disc storage using an ARL-designed stand-alone controller, which also controlled the program halts and damage monitoring system. The FALSTAFF sequence is a series of load levels numbered 0 to 32, level 32 here representing maximum compressive load, and level 0 being a tensile load; the zero load condition is equivalent to level 7.53. Loads are applied in a series of 200 different flights (one program) which is repeated continuously; a typical fighter aircraft design life would therefore, be 20-40 programs. The stress level applied for level 32 (256 MPa) was determined from tests on undamaged coupons, and produced longitudinal strains of 3750$\mu\varepsilon$. This value is somewhat higher than the design strains in use for wing skins in current military aircraft, but was not considered unduly severe, since a nmber of factors, including design and operating uncertainties and changes in aircraft operating conditions inevitably lead to some areas in real aircraft experiencing service stresses higher than anticipated.

A modified FALSTAFF sequence was also generated, containing 9456 turning points per program instead of the 35766 in the full sequence; this represents a significant acceleration of fatigue testing. The approach used was to delete any two adjacent turning points where both are in the load level range 8 to 17; single turning points in this range were retained. Many similar modification techniques could have been chosen, but this one offered the advantage of retaining all major load excursions while deleting most of the load cycles occurring at low compressive loads. The effect of this modification on a typical flight is illustrated in Figure 6, the cycles deleted being marked.

2.6 Test Program to Investigate Effects of Spectrum Modification

The major part of the program used coupons containing damage 30mm in diameter, nine being tested under the full FALSTAFF sequence, and ten with the modified sequence. Specimens were drawn approximately equally from the three original panels, to permit investigation of the effect of any panel-to-panel variation (such as absence or otherwise of post-cure) on fatigue life. Tests were carried out in random order, and were continued until complete failure of the cross-section occurred. Three specimens with 20mm damage and three with 40mm damage were also tested using identical procedures and the modified load sequence.

3. Test Results

Fatigue lives obtained are listed in Table 1. Figure 7 shows the coupon lives grouped according to the load sequence used, and Figure 8 shows the same lives, grouped according to the original panel designation. A two-way analysis of variance, carried out to determine whether the fatigue lives were infuenced by either of these two factors, showed (Table 2) that at a 5% level of significance, there was a significant influence of panel-to-panel variation, while no influence could be attributed to spectrum modification. the analysis also confirmed that the

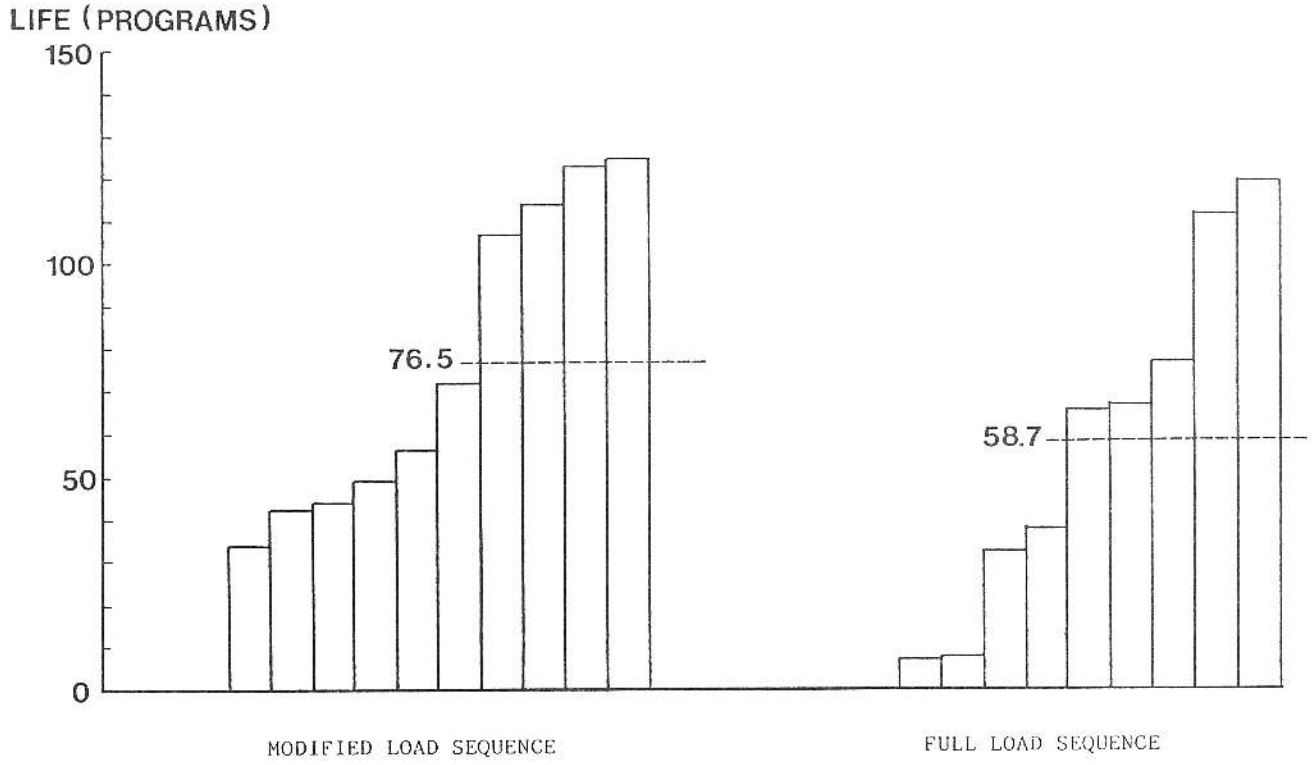

Figure 7. Specimen fatigue lives for both full and modified load sequences; mean lives of the two groups are shown.

SEQUENCE	DAMAGE SIZE (mm)	PANEL		
		FG	FH	FI
FULL FALSTAFF SEQUENCE	30	FG2 7 FG3 38 FG7 7.5	FH7 67 FH10 120 FH12 66	FI6 34 FI8 77 FI12 112
MODIFIED FALSTAFF SEQUENCE	20		FH1 505	FI5 538 FI11 386
	30	FG5 33.5 FG8 42 FG14 44	FH3 49 FH8 56 FH9 125	FI3 72 FI7 123 FI9 114 FI10 107
	40	FG1 17	FH5 69	FI4 217

Table 1: Specimen Fatigue Lives

NULL HYPOTHESIS	CALCULATED VALUE OF F	LIMITING VALUE OF F (5% LEVEL)	CONCLUSION
NO EFFECT OF MODIFICATION ON FAT. LIFE	3.13	6.2	ACCEPT
NO EFFECT OF PANEL-TO-PANEL VARIATION ON FATIGUE LIFE	10.61	4.8	REJECT

Table 2: Results of Two-Way Analysis of Variance

panel-to-panel effect (Figure 8) was caused by low values of fatigue life for specimens cut from panel FG, which had not been post-cured.

Figure 9 shows a series of shadow Moire interference fringe patterns photographed at stages during the life of specimen FH1. The progression of the delamination damage shown is typical of these tests; damage grows across the specimen, rather than along the length (0 degree fiber direction), maintaining an approximately rectangular shape.

Figure 10 shows the change in delamination width during tests on coupons containing 30mm damage (Figure 10a) and 20mm and 40mm damage (Figure 10b). These curves are a best-fit representation of the data, and were differentiated at a number of points to determine the damage growth rates which are shown in Figure 11 as a function of delamination width. In some cases (e.g. specimen FH1, where a "stepped" form of growth was observed) it was not possible to derive reliable growth rate data. The results in Figure 11 can be seen to fall into a well-defined band, indicating increasing growth rates as the damage progresses.

4. Discussion

The conditions under which damage may be introduced in CFC aircraft components vary widely, and the impact damage used in these tests is necessarily a somewhat idealised case, since the clamping arrangement limited damage size. However,

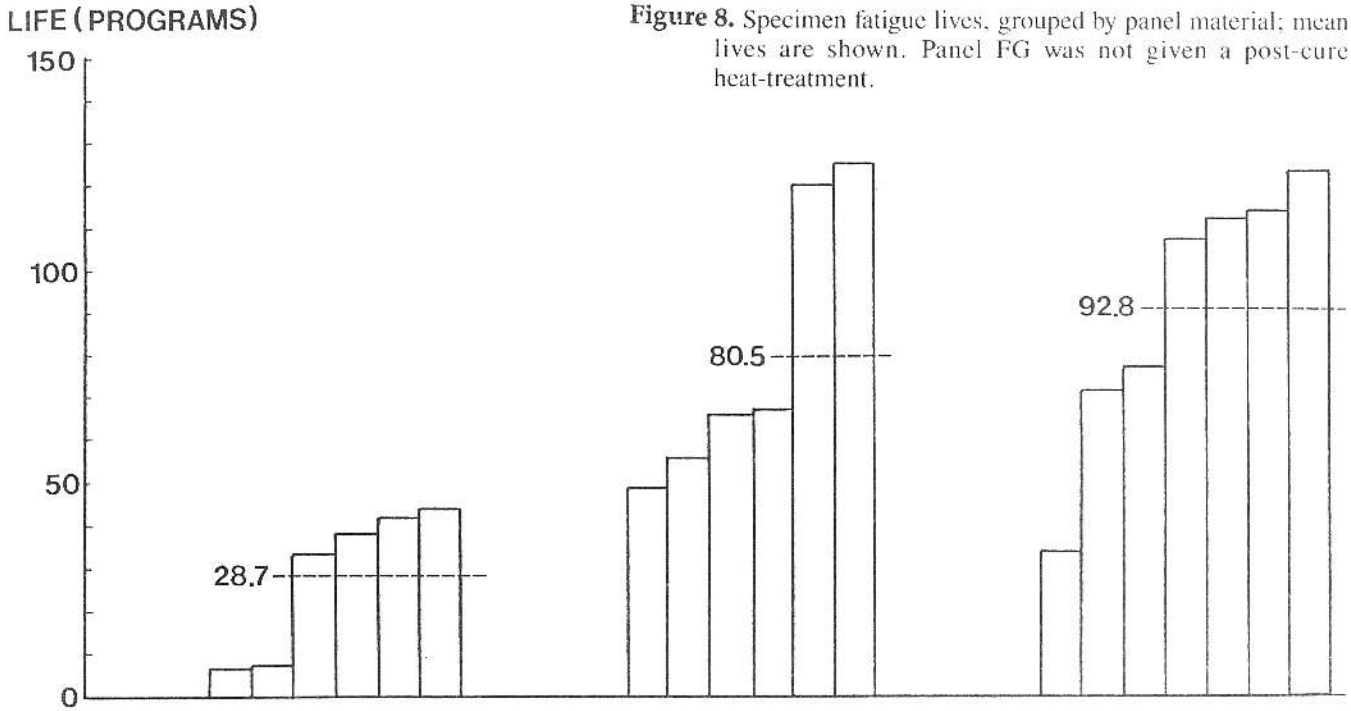

Figure 8. Specimen fatigue lives, grouped by panel material; mean lives are shown. Panel FG was not given a post-cure heat-treatment.

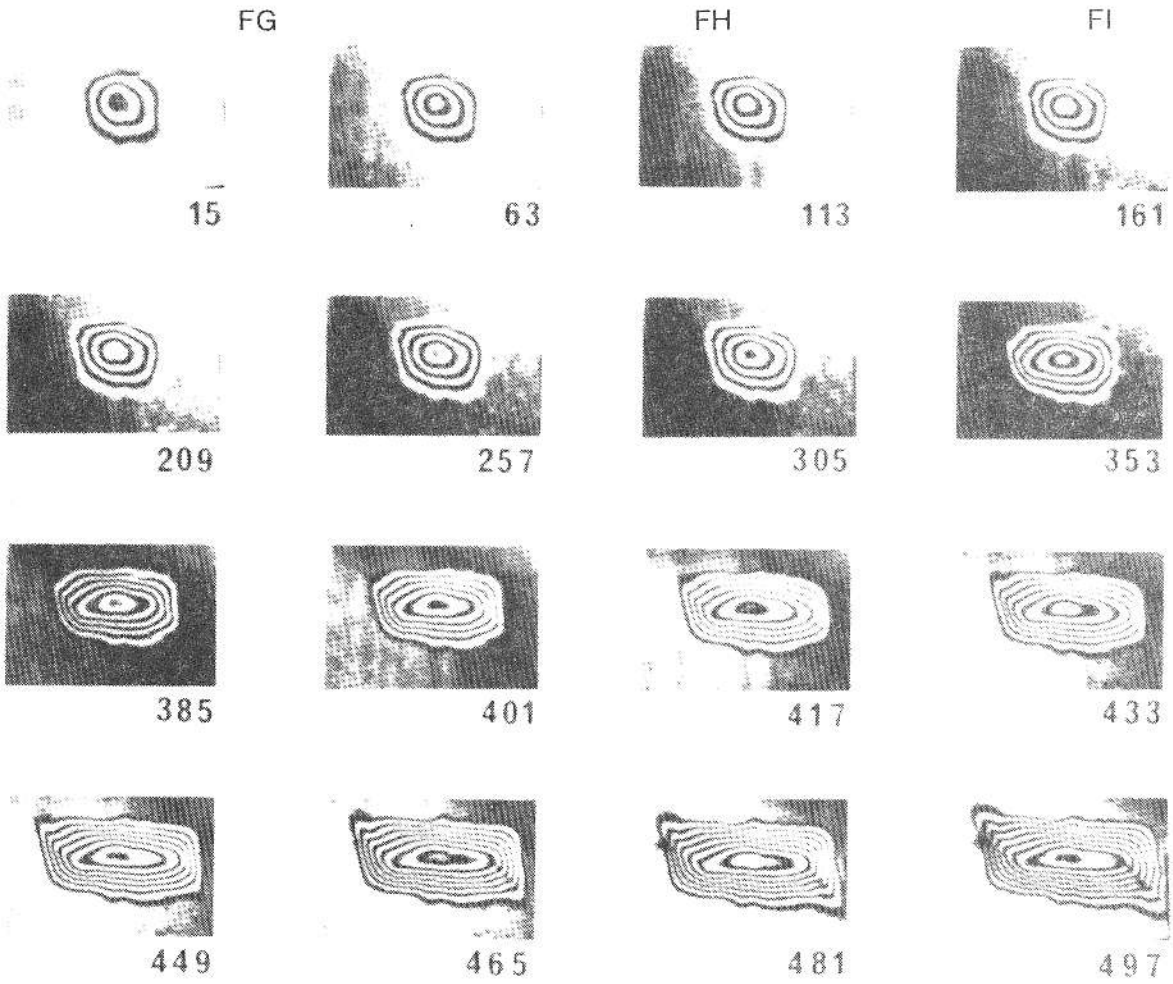

Figure 9. Shadow Moire interference fringes, indicating growth of damage in specimen FHI. The number of programs completed at each stage is indicated.

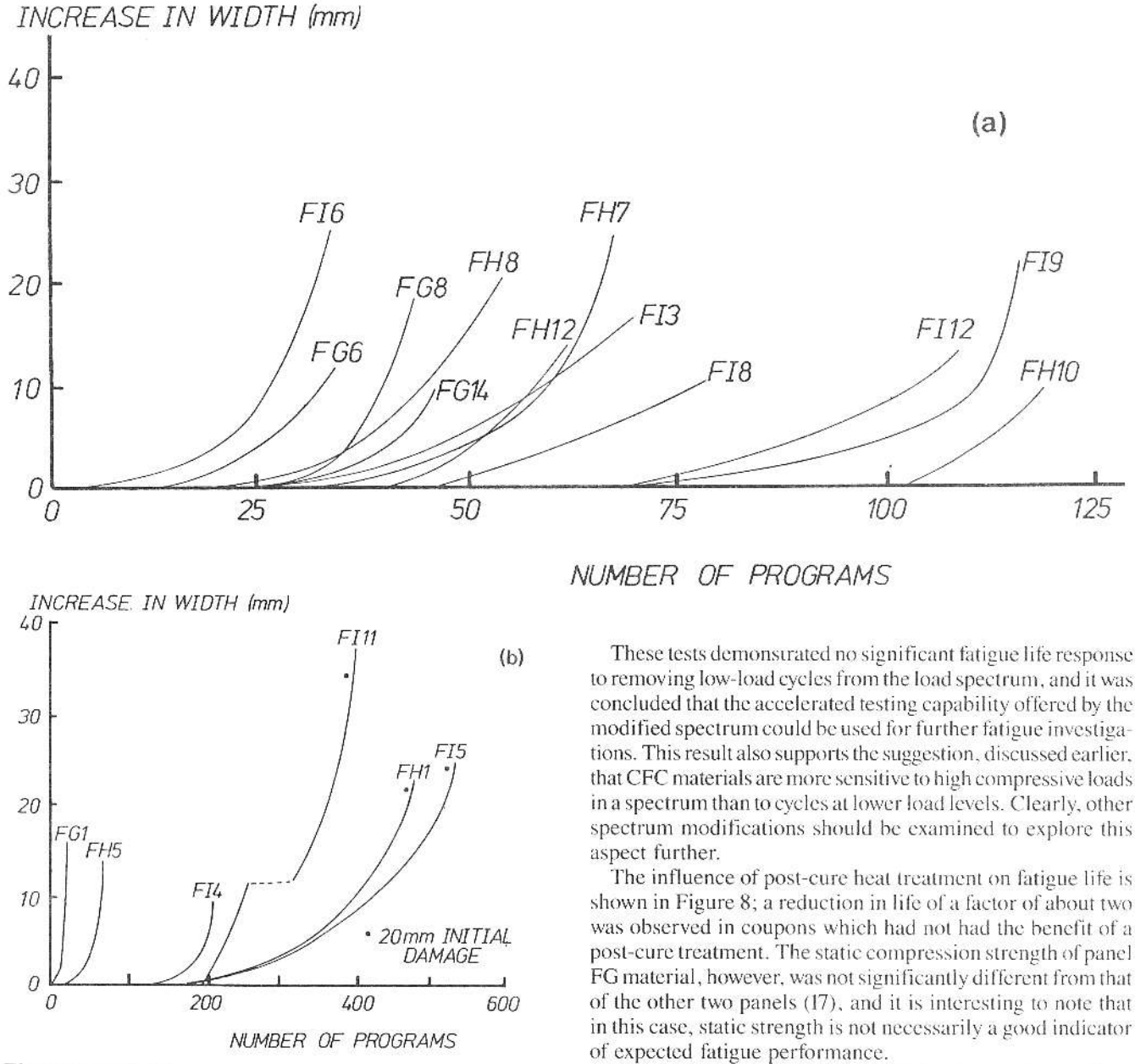

Figure 10. (a) (b)

Damage width as a function of number of fatigue programs (a) 30mm initial damage (b) 20mm or 40mm initial damage size.

since the damage cross-sections shown in Figure 3 are very similar to those observed by the authors in less highly constrained tests (11), and the impact energy is realistic, the damage used in the present tests is throught to be a reasonable representation of what might occur in a CFC wing skin in a more highly constrained region such as the corner of a bay. Furthermore, since the material used is typical of an aircraft wing skin, and the loading used, although severe, is realistic, it can be concluded that growth of impact damage by fatigue could occur in highly-stressed parts of an aircraft structure; this should be considered prior to any future increase in the allowable design strains for CFC components.

These tests demonstrated no significant fatigue life response to removing low-load cycles from the load spectrum, and it was concluded that the accelerated testing capability offered by the modified spectrum could be used for further fatigue investigations. This result also supports the suggestion, discussed earlier, that CFC materials are more sensitive to high compressive loads in a spectrum than to cycles at lower load levels. Clearly, other spectrum modifications should be examined to explore this aspect further.

The influence of post-cure heat treatment on fatigue life is shown in Figure 8; a reduction in life of a factor of about two was observed in coupons which had not had the benefit of a post-cure treatment. The static compression strength of panel FG material, however, was not significantly different from that of the other two panels (17), and it is interesting to note that in this case, static strength is not necessarily a good indicator of expected fatigue performance.

The standard deviation of log life for the specimens from panels FH and FI was found to be 0.18. This is an important result, since it indicates that careful control of experimental conditions makes it possible to keep the scatter down to values comparable with results for metals testing.

The way in which damage growth proceeds across the specimen (Figure 9) with only a small growth component in the longitudinal (0 degree fiber) direction is of interest. This behaviour may be associated with the absence of 90 degree fibers in this lay-up; in many aircraft components, however, a small number of 90 degree plies are included to provide improved biaxial elastic properties, and this type of growth behaviour may not be observed in such cases. Another aspect of the growth process is that it is clearly discontinuous, as shown in Figure 10b, where there is a long delay in damage growth in specimen FI11. Similar, but less pronounced behaviour, was also observed in other specimens. The deterioration process occurring between periods of damage growth is not known, and may be resolved in further work.

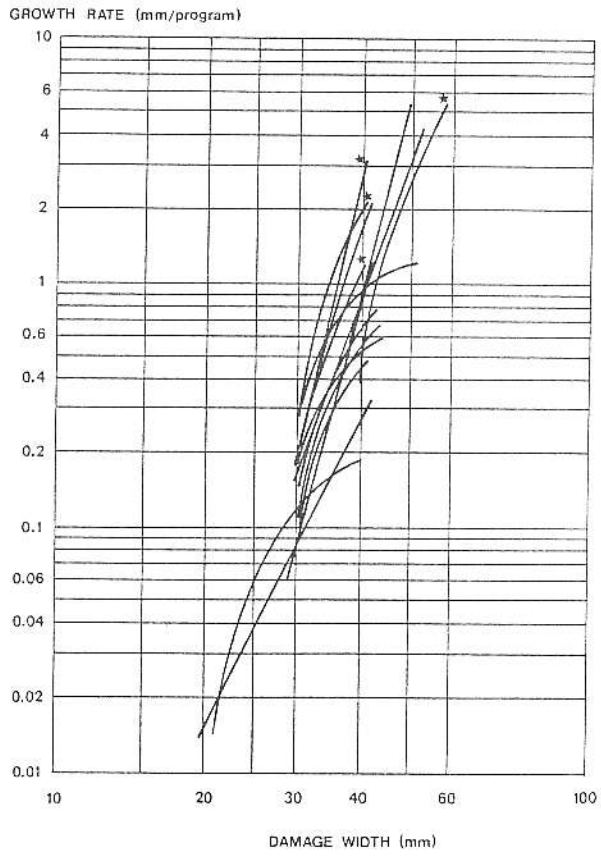

Figure 11.

Damage growth rate, as a function of damage width for 20, 30 and 40mm initial damage sizes. Results marked * are from coupons from panel FG.

The damage growth rate curve in Figure 11 is extremely encouraging, in that a clearly-defined and fairly consistent materials behaviour could be derived. Indeed, the scatter in growth rates is smaller than might have been expected, given the high level of scatter observed in most composites properties, and the complexity of the experimental techniques used. A major conclusion from the data in Figure 11 is that growth rate is controlled in this case by damage width, although further experimental work at other stress levels is really required to provide a broader data base. Such work should also make it possible to examine a range of empirical parameters which are functions of both stress and damage size, and hence perhaps determine a more useful relationship similar to the growth rate-ΔK relationships which are well established for metals.

5. Conclusions

The conclusions listed below are drawn from the results of the test program. It is important to note that these conclusions are necessarily specific to the material and lay-up tested, and relate only to uniaxial loading; in glider wings, biaxial stresses are important, and further extension of this type of work to biaxial loading is considered important.

5.1 Low-level impact damage can propagate to failure by compression-dominated fatigue under severe aircraft wing skin loading conditions.

5.2 Damage growth normal to the 0 degree fiber direction was pronounced; little growth was observed in the 0 degree fiber direction.

5.3 Damage growth rate was controlled by damage width, apparently independently of initial damage area.

5.4 Load spectrum modification by removal of low-load cycles is an acceptable means of accelerating fatigue tests; damage growth is insensitive to the presence of these load cycles.

5.5 Variations in material processing can have a significant effect on damage growth. Specifically, omission of a post-cure heat-treatment reduced fatigue life by a factor of approximately two, while having no significant effect on static strength.

5.6 With careful control of impact-damage conditions and test methods, the scatter observed in fatigue life can be similar to that seen in metals testing.

5.7 The addition of further damage growth rate data at different stress levels would make it possible to assess a range of empirical parameters which could control damage growth in fatigue.

6. Acknowledgements

The authors would like to acknowledge the assistance of Mr. T.E. Preuss, Mr. J. D. Roberts and Mr. B. Lawrie of A.R.L. with this work.

7. References

(1) A.A. Baker, R. Jones and R.J. Callinan. (1985) Damage Tolerance of Grphite/Epoxy Composites. Composite Structures, 4, 15-44.

(2) R. Jones, J. Paul and W. Broughton. (1948) On the effects of delamination damage in fiber composite laminates. Struct. Rpt. 403, Aeronautical Res. Laboratories.

(3) M.M. Ratwani and H.P. Kan. (1979) Compression fatigue analysis of fiber composites. Report NADC-78049-69, Naval Air Development Center.

(4) A.S.D. Wang and F.W. Crossman. (1980) Initiation and growth of transverse cracks and delaminations. J. Composite Materials, 14, 71-87.

(5) S.S. Wang. (1982) Fracture mechanics for delamination problems in composite materials. Proc. Intl. Conf. Composite Materials IV, vol. 1, 287-296.

(6) R. Jones and R.J. Callinan. (1982) Analysis of compression failures in composite materials, ibid, pp. 447-454.

(7) F.W. Crossman, W.J. Warren, A.S.D. Wang and G.E. Law. (1980) Initiation and growth of transverse cracks and edge delaminations in composite materials, part 2. J. Composite Materials, 14, 87.

(8) M.S. Rosenfeld and L.W. Gause. (1981) Compression fatigue behaviour of graphite epoxy in the presence of stress raisers. Special Technical Publication 723, American Society for Testing and Materials.

(9) R.T. Potter. (1983) The significance of defects and damage in composite structures. AGARD Conf. Characterisation Analysis and significance of Defects in Composite Materials, AGARD-CP-355.

(10) W. Geier. J. Vilismeier and D. Weiserber. (1983) Experimental investigation of delamination in carbon. ibid.

(11) G. Clark and T.J. van Blaricum. Carbon fiber composite coupons — static and fatigue behaviour after impact damage. Structures Report in preparation, Aeronautical Research Laboratories, Melbourne.

(12) R.L. Ramkumar. (1983) Effect of low-velocity impact on the fatigue behaviour of graphite/epoxy laminates. Special Technical Publication 813, American Society for Testing and Materials.

(13) E. Demuts and R.E. Horton. (1985) Damage tolerant composite design development. Composite Structures 3, ed. I.H. Marshall, Elsevier, London.

(14) J.R. Heath-Smith. (1979) Theoretical considerations in the use of FALSTAFF loading for fatigue research in carbon fiber composite. Technical Report 79124, Royal Aircraft Establishment.

(15) T.E. Preuss. Ultrasonic depth C-scanning of carbon fiber composite coupons. Technical Memorandum in preparation, Aeronautical Research Laboratories.

(16) W.R. Broughton and R.J. Chester. The development of a portable ultrasonic facility for NDI of graphite/epoxy composites. J.Aust.Inst. NDT (in press).

(17) T.J. van Blaricum. Effect of inadequate post-cure on static and fatigue behaviour of carbon-fiber composite panels. Structures Technical Memorandum in preparation, Aeronautical Research Laboratories, Melbourne.

(18) H. Lowak, M. Huck, D. Schutz and W. Schutz. (1976) Standardisiertes Einzelflugprogramm fur Kampfflugzeuge FALSTAFF. Rpt 3045, Laboratorium fur Betriebsfestigkeit.